

Radiative Corrections to $H^0 \rightarrow WW/ZZ$ in the MSSM

Wolfgang Hollik^a and Jian-Hui Zhang^{a,b}

^a*Max-Planck-Institut für Physik,
Föhringer Ring 6, 80805 München, Germany*

^b*Center for High Energy Physics,
Peking University, Beijing, China*

Abstract

The electroweak $\mathcal{O}(\alpha)$ radiative corrections to the decay of the heavy CP-even MSSM Higgs boson to weak gauge bosons are presented. Due to the suppression of the tree-level $H^0 WW/H^0 ZZ$ coupling, the electroweak contributions to the partial decay width are significant. Although the effective Born decay width can be rather small for certain M_{A^0} values (especially for large $\tan\beta$), the corrected partial widths at different values of M_{A^0} are of comparable size.

1 Introduction

One of the major tasks of the Large Hadron Collider (LHC) at CERN is to explore the mechanism responsible for the electroweak symmetry breaking (EWSB). In the standard model (SM), the EWSB is realized by the Higgs mechanism, which predicts the existence of a physical scalar boson, the Higgs boson. The mass of the Higgs boson cannot be predicted by the SM. Experimental searches at LEP [1] and Tevatron [2] have excluded a Higgs mass $M_H < 114.4 \text{ GeV}$ and $158 \text{ GeV} < M_H < 173 \text{ GeV}$, both at 95% confidence level (C.L.). In addition, electroweak precision analysis favors a relatively light SM Higgs boson with a mass $M_H < 158 \text{ GeV}$ (or $M_H < 185 \text{ GeV}$ if the LEP2 direct search limit is included) [3].

In the minimal supersymmetric standard model (MSSM), which is the most economic extension of the SM that incorporates supersymmetry, two complex Higgs doublets are required for consistency. After the EWSB, three of the eight degrees of freedom are absorbed by the weak gauge bosons and become their longitudinal components, leading to five physical Higgs bosons, h^0 and H^0 (CP-even), A^0 (CP-odd) and H^\pm (charged). At tree-level the Higgs sector of MSSM can be described by two parameters, which can be chosen as M_{A^0} and $\tan\beta$, where M_{A^0} is the mass of the CP-odd Higgs boson and $\tan\beta$ is the ratio of the vacuum expectation values of the two Higgs doublets. The tree-level mass of the light CP-even Higgs boson is bounded from above by the mass of Z boson as a consequence of supersymmetry. Dependence of the Higgs sector on parameters of other sectors enters via radiative corrections. By including radiative corrections (up to two-loop order), the upper mass bound of the light CP-even Higgs boson is shifted to $\sim 135 \text{ GeV}$ [4, 7, 8].

It is interesting to investigate the behavior of the MSSM Higgs sector in the decoupling limit $M_{A^0} \gg M_Z$ [9]. In this limit, the heavy CP-even Higgs boson H^0 and the charged Higgs bosons H^\pm are nearly degenerate in mass with A^0 , and the coupling of the light CP-even Higgs boson to SM fermions and gauge bosons resembles the corresponding coupling for the SM Higgs boson. If only one light Higgs boson is discovered, it might be compatible both with the SM and with the MSSM. If there are extra heavy Higgs bosons observed, they would indicate the incompleteness of the SM. Investigating the decay properties of such heavy Higgs bosons can then help disentangle supersymmetry from other potential extensions of the SM with an extended Higgs sector.

In the MSSM, the tree-level coupling of the heavy CP-even Higgs boson to gauge bosons is suppressed by a factor of $\cos(\beta - \alpha)$, compared to the corresponding coupling for the SM Higgs boson, where α is the angle that diagonalizes the CP-even Higgs sector at tree-level. This suppression can be rather strong for large values of M_{A^0} , hence it is of particular interest to investigate the impact of radiative corrections in such situations.

In this paper we consider the electroweak radiative corrections to the decay of the heavy CP-even Higgs boson to weak gauge bosons. Electroweak corrections can induce important modifications to the tree-level $H^0 WW/H^0 ZZ$ coupling. One potential source of large corrections is the contribution of loops involving fermions and sfermions, and in particular of loops involving the third generation fermions and sfermions, since they contain potentially large Yukawa couplings. The Higgs propagator corrections can give rise to significant contributions as well. In this work we concentrate on CP-conserving MSSM with real parameters, therefore the heavy CP-even Higgs boson can only mix with the light CP-even one.

The outline of this paper is as follows. In section 2 we discuss the structure of the $H^0 WW/H^0 ZZ$ vertex correction. In section 3 the decay amplitudes of H^0 to WW/ZZ are given. Section 4 is devoted for numerical discussions. We draw our conclusions in section 5.

2 Corrections to the $H^0 WW/H^0 ZZ$ vertices

2.1 Correction to the $H^0 WW$ vertex

The tree-level $H^0 WW$ coupling is given by

$$V_{H^0,0}^{\mu\nu} = \frac{eM_W}{s_W} \cos(\beta - \alpha) g^{\mu\nu} \equiv V_{H^0} \cos(\beta - \alpha) g^{\mu\nu} , \quad (1)$$

where V_{H^0} denotes the coupling of the SM Higgs boson to W bosons. When the mass of the CP-odd Higgs boson M_{A^0} becomes large, the angle $\beta - \alpha \rightarrow \pi/2$ and the factor $\cos(\beta - \alpha)$ approaches 0 as $\mathcal{O}(M_Z^2/\sin 4\beta/M_{A^0}^2)$, thus the tree-level coupling is strongly suppressed.

The one-loop corrected $H^0 WW$ vertex possesses the following structure [11]

$$\begin{aligned} V_{H^0}^{\mu\nu} &= V_{H^0,0}^{\mu\nu} + V_{H^0,1}^{\mu\nu} \\ &= V_{H^0,0}^{\mu\nu} + V_{H^0} (A k_2^\mu k_2^\nu + B k_3^\mu k_3^\nu + C k_2^\mu k_3^\nu + D k_3^\mu k_2^\nu + E g^{\mu\nu} - i F \varepsilon^{\mu\nu\rho\sigma} k_{2\rho} k_{3\sigma}) , \end{aligned} \quad (2)$$

where k_2, k_3 denote the momenta of the two gauge bosons, $\varepsilon^{\mu\nu\rho\sigma}$ is totally antisymmetric with $\varepsilon^{0123} = 1$. If the gauge bosons are on-shell, then only D and E terms will contribute. As mentioned in the introduction, the loop contributions from the fermionic and sfermionic sector, and in particular from the third generation fermions and sfermions are expected to be sizable. In Fig. 1 we show as examples the Feynman diagrams involving fermion and sfermion loops. The packages FeynArts [13], FormCalc [16] and LoopTools [19] are used throughout the computation.

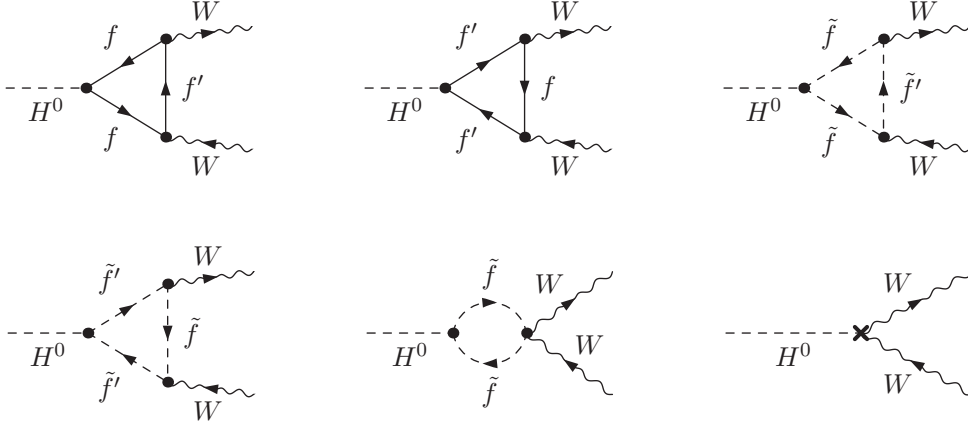


Figure 1: One-loop vertex diagrams and counter term diagram for $H^0 WW$.

The contribution of the vertex counter term diagram in Fig. 1 can be written as (see *e.g.* [20])

$$V_{H^0,CT}^{\mu\nu} = V_{H^0,0}^{\mu\nu} \left[\delta Z_e + \delta Z_W + \frac{1}{2} \frac{\delta M_W^2}{M_W^2} + \frac{\delta s_W}{s_W} + \frac{\sin(\beta - \alpha)}{\cos(\beta - \alpha)} (-\cos^2 \beta \delta \tan \beta + \frac{1}{2} \delta Z_{h^0 H^0}) + \frac{1}{2} \delta Z_{H^0 H^0} \right], \quad (3)$$

where δZ_e is the charge renormalization constant, δZ_W is the field renormalization constant for the W boson, and δM_W^2 the mass counter term for the W boson. δs_W is the renormalization constant for the weak mixing angle. $\delta Z_{h^0 H^0}$ and $\delta Z_{H^0 H^0}$ are the Higgs field renormalization constants in the mass eigenstate basis. The counter term for $\tan \beta$ is introduced via $\tan \beta \rightarrow \tan \beta + \delta \tan \beta$. The vertex counter term is proportional to the tree-level coupling, and thus contributes to the E -term in Eq. (2).

To determine the Higgs field renormalization constants, we choose the \overline{DR} scheme [21]. In this scheme, the Higgs field renormalization constants are given by

$$\begin{aligned} \delta Z_{h^0 h^0} &= -[\text{Re } \Sigma'_{h^0 h^0}(m_{h^0}^2)]^{\text{div}}, \\ \delta Z_{H^0 H^0} &= -[\text{Re } \Sigma'_{H^0 H^0}(m_{H^0}^2)]^{\text{div}}, \\ \delta Z_{h^0 H^0} &= \delta Z_{H^0 h^0} = \frac{\sin \alpha \cos \alpha}{\cos 2\alpha} (\delta Z_{h^0 h^0} - \delta Z_{H^0 H^0}), \end{aligned} \quad (4)$$

where m_{h^0} , m_{H^0} denote the tree-level masses of the two CP-even Higgs bosons, "div" means we only take into account the divergent parts of the renormalization constants. The counter term $\delta \tan \beta$ is fixed by

$$\frac{\delta \tan \beta}{\tan \beta} = \left(\frac{\delta \tan \beta}{\tan \beta} \right)^{\overline{DR}} = \frac{1}{2 \cos 2\alpha} (\delta Z_{h^0 h^0} - \delta Z_{H^0 H^0}). \quad (5)$$

For the renormalization scale, we choose $\mu^{\overline{DR}} = m_t$. The remaining counter terms in Eq. (3) are

fixed in the on-shell scheme as follows [22]

$$\begin{aligned}
\delta Z_e &= \frac{1}{2} \Sigma'_\gamma(0) - \frac{s_W}{c_W} \frac{\Sigma_{\gamma Z}^T(0)}{M_Z^2} , \\
\delta Z_W &= -\text{Re} \Sigma_W'^T(M_W^2) , \\
\delta M_W^2 &= \text{Re} \Sigma_W^T(M_W^2) , \\
\delta M_Z^2 &= \text{Re} \Sigma_Z^T(M_Z^2) , \\
\frac{\delta s_W}{s_W} &= \frac{1}{2} \frac{c_W^2}{s_W^2} \left(\frac{\delta M_Z^2}{M_Z^2} - \frac{\delta M_W^2}{M_W^2} \right) ,
\end{aligned} \tag{6}$$

where the prime indicates the derivative and the superscript T denotes the transverse part of the corresponding self energy.

Due to the mixing between the two CP-even Higgs bosons beyond tree-level, when evaluating the radiative corrections to the decay $H^0 \rightarrow WW$ we need to take into account the $h^0 WW$ vertex correction as well. The tree-level $h^0 WW$ coupling is simply obtained by replacing $\cos(\beta - \alpha)$ in Eq. (1) with $\sin(\beta - \alpha)$, and the corresponding counter term contribution reads

$$\begin{aligned}
V_{h^0,CT}^{\mu\nu} &= V_{H^0} \sin(\beta - \alpha) g^{\mu\nu} \left[\delta Z_e + \delta Z_W + \frac{1}{2} \frac{\delta M_W^2}{M_W^2} + \frac{\delta s_W}{s_W} + \frac{\cos(\beta - \alpha)}{\sin(\beta - \alpha)} (\cos^2 \beta \delta \tan \beta \right. \\
&\quad \left. + \frac{1}{2} \delta Z_{H^0 h^0}) + \frac{1}{2} \delta Z_{h^0 h^0} \right] ,
\end{aligned} \tag{7}$$

where the field renormalization constants $\delta Z_{h^0 h^0}$ and $\delta Z_{H^0 h^0}$ are given in Eq. (4).

2.2 Correction to the $H^0 ZZ$ vertex

The tree-level $H^0 ZZ$ coupling has the same structure as the tree-level $H^0 WW$ coupling

$$V_{H^0,0}'^{\mu\nu} = \frac{e M_W}{c_W^2 s_W} \cos(\beta - \alpha) g^{\mu\nu} \equiv V_{H^0}' \cos(\beta - \alpha) g^{\mu\nu} , \tag{8}$$

it also differs from the SM counterpart by a factor of $\cos(\beta - \alpha)$ and gets strongly suppressed in the decoupling limit $M_{A^0} \gg M_Z$.

The corrected vertex has the same tensor structure as in Eq. (2), with V_{H^0} replaced by V_{H^0}' . The corresponding counter term contributions are given by

$$\begin{aligned}
V_{H^0,CT}'^{\mu\nu} &= V_{H^0,0}'^{\mu\nu} \left[\delta Z_e + \delta Z_Z + \frac{1}{2} \frac{\delta M_W^2}{M_W^2} - \frac{\delta s_W}{s_W} (2 \frac{s_W^2}{c_W^2} - 1) + \frac{\sin(\beta - \alpha)}{\cos(\beta - \alpha)} (-\cos^2 \beta \delta \tan \beta \right. \\
&\quad \left. + \frac{1}{2} \delta Z_{h^0 H^0}) + \frac{1}{2} \delta Z_{H^0 H^0} \right] ,
\end{aligned} \tag{9}$$

and

$$\begin{aligned}
V_{h^0,CT}'^{\mu\nu} &= V_{H^0}' \sin(\beta - \alpha) g^{\mu\nu} \left[\delta Z_e + \delta Z_Z + \frac{1}{2} \frac{\delta M_W^2}{M_W^2} - \frac{\delta s_W}{s_W} (2 \frac{s_W^2}{c_W^2} - 1) \right. \\
&\quad \left. + \frac{\cos(\beta - \alpha)}{\sin(\beta - \alpha)} (\cos^2 \beta \delta \tan \beta + \frac{1}{2} \delta Z_{H^0 h^0}) + \frac{1}{2} \delta Z_{h^0 h^0} \right] ,
\end{aligned} \tag{10}$$

with $\delta Z_Z = -\text{Re} \Sigma_Z'^T(M_Z^2)$.

3 Decay amplitudes of $H^0 \rightarrow WW/ZZ$

The decay amplitude can be obtained from the coupling vertex in the previous section by putting all external momenta on-shell and multiplying with the polarization vectors for the external gauge bosons. Beyond the lowest order, the CP-even Higgs propagator matrix receives important radiative corrections, leading to finite wave function normalization factors for the external Higgs boson. These wave function normalization factors can be incorporated by using the following effective Born amplitude

$$\begin{aligned}\mathcal{M}_{\text{eff}}^0 &= \sqrt{Z_{H^0}}(\mathcal{M}_{H^0}^0 + Z_{H^0 h^0} \mathcal{M}_{h^0}^0) \\ &= \sqrt{Z_{H^0}} \mathcal{M}_{H^0}^0 (1 + \tan(\beta - \alpha) Z_{H^0 h^0}) ,\end{aligned}\quad (11)$$

where $\mathcal{M}_{H^0}^0$ and $\mathcal{M}_{h^0}^0$ denote the tree-level decay amplitude for H^0 and h^0 , respectively. For illustrating purposes, we will present in the next section both the tree-level results obtained from $\mathcal{M}_{H^0}^0$ and the effective tree-level results obtained from $\mathcal{M}_{\text{eff}}^0$. The wave function normalization factors Z_{H^0} and $Z_{H^0 h^0}$ in Eq. (11) can be determined from the renormalized self energies of Higgs bosons as

$$\begin{aligned}Z_{H^0} &= \frac{1}{1 + \text{Re} \hat{\Sigma}'_{H^0}(k^2) - \text{Re} \left(\frac{\hat{\Sigma}_{h^0 H^0}^2(k^2)}{k^2 - m_{h^0}^2 + \hat{\Sigma}_{h^0}(k^2)} \right)' \Big|_{k^2=M_{H^0}^2}} , \\ Z_{H^0 h^0} &= - \frac{\hat{\Sigma}_{h^0 H^0}(M_{H^0}^2)}{M_{H^0}^2 - m_{h^0}^2 + \hat{\Sigma}_{h^0}(M_{H^0}^2)} ,\end{aligned}\quad (12)$$

where M_{H^0} is the physical mass of H^0 . In this work the physical masses of Higgs bosons and the finite wave function normalization factors are computed with the program package FeynHiggs [23], in which the dominant two-loop corrections to the Higgs boson self energies are also taken into account. For the decay to W bosons, $\mathcal{M}_{H^0}^0$ is given by

$$\mathcal{M}_{H^0}^0 = V_{H^0,0}^{\mu\nu} \epsilon_\mu \epsilon_\nu , \quad (13)$$

where $V_{H^0,0}^{\mu\nu}$ is defined in Eq. (1) and $\epsilon_{\mu,\nu}$ are the polarization vectors of the external W bosons. The amplitude for the decay of H^0 to Z bosons can be obtained analogously.

At one-loop level, one can also write an effective amplitude

$$\mathcal{M}_{\text{eff}}^1 = \sqrt{Z_{H^0}}(\mathcal{M}_{H^0}^1 + Z_{H^0 h^0} \mathcal{M}_{h^0}^1) . \quad (14)$$

In the following the results obtained from this effective amplitude will be denoted as effective one-loop results. In obtaining such results we also include the square of the one-loop amplitude, since the tree-level coupling can be suppressed so that the square of the one-loop amplitude can become comparable to the tree-level result. For the decay $H^0 \rightarrow WW$, we compute the complete $\mathcal{O}(\alpha)$ contributions, and the effective one-loop contributions from the fermionic and sfermionic loops, which do not involve infrared divergences. For the decay $H^0 \rightarrow ZZ$, we compute also the complete effective one-loop contribution as the complete one-loop amplitude is infrared finite in this case.

4 Numerical discussions

For the numerical evaluation, we choose the benchmark scenarios suggested in [26], where the two parameters that govern the tree-level Higgs sector, M_{A^0} and $\tan \beta$, are kept as free parameters.

The SM parameters used in the numerical analysis are the same as in ref. [28]. Throughout the parameter scan, the experimental mass exclusion limits from direct search of supersymmetric particles and the upper bound on the SUSY corrections to the electroweak ρ parameter [29] have been taken into account (except for the tree-level result). In the parameter region $50 \text{ GeV} < M_{A^0} < 1 \text{ TeV}$ and $1 < \tan \beta < 50$, the gluophobic scenario has been ruled out by the bound derived from the $\text{BR}(B \rightarrow X_s \gamma)$ prediction [30], therefore we will not discuss this scenario here. The investigated scenarios are listed as follows:

1. The m_h^{max} scenario

The parameters in this scenario are given by

$$\begin{aligned} M_{\text{SUSY}} &= 1 \text{ TeV} , & \mu &= 200 \text{ GeV} , & M_2 &= 200 \text{ GeV} , \\ X_t &= 2M_{\text{SUSY}} , & A_b &= A_t = A_\tau , & m_{\tilde{g}} &= 0.8M_{\text{SUSY}} , \end{aligned} \quad (15)$$

where M_{SUSY} is the soft SUSY-breaking parameter, μ is the supersymmetric Higgs mass parameter, M_2 denotes the $SU(2)$ gaugino mass, X_t the mixing parameter of the top squark sector, $A_{b,t,\tau}$ the trilinear couplings for the third generation squark and slepton and $m_{\tilde{g}}$ the gluino mass. This scenario yields a maximal value of the lightest CP-even Higgs boson mass for given M_{A^0} and $\tan \beta$.

2. The no-mixing scenario

The only difference of this scenario from the m_h^{max} scenario is the vanishing mixing in the top squark sector and a higher value of M_{SUSY} , where the latter is chosen to avoid the exclusion bounds from the LEP Higgs searches [1, 31]. The parameters in this scenario read

$$\begin{aligned} M_{\text{SUSY}} &= 2 \text{ TeV} , & \mu &= 200 \text{ GeV} , & M_2 &= 200 \text{ GeV} , \\ X_t &= 0 , & A_b &= A_t = A_\tau , & m_{\tilde{g}} &= 0.8M_{\text{SUSY}} . \end{aligned} \quad (16)$$

3. The small- α_{eff} scenario

In this scenario a suppression of the $h^0 b \bar{b}$ coupling can occur. The parameters are given by

$$\begin{aligned} M_{\text{SUSY}} &= 800 \text{ GeV} , & \mu &= 2.5M_{\text{SUSY}} , & M_2 &= 500 \text{ GeV} , \\ X_t &= -1100 \text{ GeV} , & A_b &= A_t = A_\tau , & m_{\tilde{g}} &= 500 \text{ GeV} . \end{aligned} \quad (17)$$

To illustrate the numeric impact of radiative corrections, we show in Fig. 2 and 3 the dependence on M_{A^0} of the lowest order and the corrected partial decay widths in the m_h^{max} scenario for $\tan \beta = 5, 30$. As can be seen by comparing the tree-level and the effective Born results in the figures, the contributions of Higgs propagator corrections are significant, they change the dependence of the tree-level result on M_{A^0} dramatically. An interesting feature of the effective Born results is that they reach a minimum for moderate M_{A^0} values ($\sim 420/500 \text{ GeV}$ depending on $\tan \beta$). This is due to the cancellation of the two parts in the effective Born amplitude Eq. (11) at such values of M_{A^0} . As shown in the figures, the tree-level partial decay width for $\tan \beta = 30$ is much smaller than that for $\tan \beta = 5$, since for relatively large M_{A^0} , the tree-level coupling of H^0 to vector boson pair is suppressed by $\tan \beta$ as well, as explained in the discussions below Eq. (1). For $H^0 \rightarrow WW$, at $\tan \beta = 5$ the contribution of the fermionic and sfermionic sector yields the dominant part of the $\mathcal{O}(\alpha)$ corrections, and the leading contribution from the fermionic and sfermionic sector is that from the third generation fermions and sfermions. For $\tan \beta = 30$, besides the fermionic and sfermionic contribution, the contribution from other sectors to $\mathcal{O}(\alpha)$ corrections are also important. In Fig. 2 we also show the effective one-loop results with fermionic and sfermionic loop contributions (corrections beyond $\mathcal{O}(\alpha)$ described in Sec. 3 are included), from which one can see again that the third generation fermionic and sfermionic contribution yields the leading contribution of the fermionic and sfermionic sector. For $\tan \beta = 5$, the relative difference

between the effective one-loop results and the $\mathcal{O}(\alpha)$ ones is less than 50% in the plotted region. For $\tan\beta = 30$, the relative difference between the effective one-loop results and the $\mathcal{O}(\alpha)$ ones is less than 50% only for small to moderate M_{A^0} values, it can go beyond 100% for large M_{A^0} values and reaches $\sim 200\%$ for $M_{A^0} = 800$ GeV, as a consequence of the strong suppression of the tree-level coupling by both $\tan\beta$ and M_{A^0} .

Fig. 3 depicts the partial decay width for $H^0 \rightarrow ZZ$. The decay width falls off rapidly when M_{A^0} goes below ~ 200 GeV, this is because for such M_{A^0} values, the Higgs boson mass is just above the production threshold of the Z boson bosons, hence the result is strongly suppressed by the available phase space. As in the decay of $H^0 \rightarrow WW$, for $\tan\beta = 5$ the fermionic and sfermionic contribution comprises the dominant part of the $\mathcal{O}(\alpha)$ corrections, while for $\tan\beta = 30$ the contribution from other sectors becomes important. The relative difference between the effective one-loop results and the $\mathcal{O}(\alpha)$ ones is less than 50% in the plotted region for $\tan\beta = 5$. For $\tan\beta = 30$ the effective one-loop results including the fermionic and sfermionic loop contribution differ significantly from the corresponding $\mathcal{O}(\alpha)$ ones at large M_{A^0} values, but the difference between the complete effective one-loop result and the complete $\mathcal{O}(\alpha)$ result is smaller, with a relative size less than 50% when $M_{A^0} \lesssim 550$ GeV (it reaches 100% for $M_{A^0} \sim 800$ GeV). Fig. 2 and 3 show that although the effective Born decay width can be rather small for certain M_{A^0} values (especially for large $\tan\beta$), the one-loop corrected widths for different values of M_{A^0} turn out to be of comparable size.

Fig. 4 and 5 show the lowest order and the corrected partial decay widths of $H^0 \rightarrow WW$ and $H^0 \rightarrow ZZ$ as a function of $\tan\beta$ in the m_h^{\max} scenario for $M_{A^0} = 200, 500$ GeV. For both M_{A^0} values, the partial decay width decreases with $\tan\beta$. As in previous plots, the leading contribution from the fermionic and sfermionic sector is from the third generation fermions and sfermions. For $M_{A^0} = 200$ GeV, the fermionic and sfermionic contribution comprises the dominant part of the $\mathcal{O}(\alpha)$ corrections, while for $M_{A^0} = 500$ GeV the contribution from other sectors also becomes important. The relative difference between the (complete) effective one-loop results and the complete $\mathcal{O}(\alpha)$ ones is less than 60% for both M_{A^0} values in the figures. The fact that the partial decay width of $H^0 \rightarrow ZZ$ is smaller than that of $H^0 \rightarrow WW$ for the same values of $\tan\beta$ and M_{A^0} is due to the presence of identical particles in the ZZ final state.

In Fig. 6 we show the corrected partial decay width as well as the relative size of the radiative corrections for $H^0 \rightarrow WW$ in the M_{A^0} - $\tan\beta$ plane for three different scenarios. For the size of the width and the relative corrections see the caption of the figure. As illustrated there, in the m_h^{\max} scenario the width is rather small for large $\tan\beta$ in a wide range of M_{A^0} values. It increases when $\tan\beta$ decreases, the relative size of the loop corrections increases rapidly with M_{A^0} and exceeds the effective tree-level result when $M_{A^0} > 310 \sim 460$ GeV depending on the values of $\tan\beta$. For large values of M_{A^0} ($\tan\beta \lesssim 30$), the relative size of the loop corrections decreases with M_{A^0} and becomes negative when $M_{A^0} \sim 650$ GeV. In the no-mixing scenario, the corrected width also increases when $\tan\beta$ decreases, and the fermionic and sfermionic contributions are negative over a large fraction of the scanned parameter space. In the small- α_{eff} scenario, the corrected decay width increases when $\tan\beta$ decreases unless when both M_{A^0} and $\tan\beta$ are large, where the partial decay width is significantly increased by the Higgs propagator corrections. The relative correction is negative in the scanned M_{A^0} - $\tan\beta$ plane except in the upper-left corner. At large $\tan\beta$ values, the relative size of the loop corrections increases with $\tan\beta$ and exceeds 100% quite rapidly. Fig. 7 illustrates the results for $H^0 \rightarrow ZZ$ in three different scenarios. The results shown in these figures exhibit similar features to those shown in the plots for $H^0 \rightarrow WW$, but the corresponding width is smaller due to the presence of identical particles in the final state.

5 Conclusions

We have computed the electroweak $\mathcal{O}(\alpha)$ radiative corrections to the decay of the heavy CP-even MSSM Higgs boson to weak gauge bosons. Due to the suppression of the tree-level $H^0 WW/H^0 ZZ$ coupling, the electroweak contributions to the partial decay width are significant, they can easily exceed the tree-level result in certain parameter space. Although the effective Born decay width can be rather small for certain M_{A^0} values (especially for large $\tan\beta$), the corrected partial widths for different values of M_{A^0} are of comparable size. We also presented the effective one-loop results for the partial decay widths, which include corrections beyond $\mathcal{O}(\alpha)$. The numeric impact of such corrections is significant for large values of $\tan\beta$ and M_{A^0} , while it is less important for small values of $\tan\beta$, and also for large $\tan\beta$ with small to moderate M_{A^0} values.

References

- [1] **LEP Working Group for Higgs Boson Searches** Collaboration, R. Barate *et al.*, *Search for the Standard Model Higgs Boson at LEP*, *Phys. Lett.* **B565** (2003) 61–75, [[hep-ex/0306033](#)].
- [2] [CDF and D0 Collaboration], *Combined CDF and D0 Upper Limits on Standard Model Higgs Boson Production with up to 8.2 fb^{-1} of Data*, 1103.3233.
- [3] <http://lep-higgs.web.cern.ch/LEPHIGGS/papers/index.html>.
- [4] S. Heinemeyer, W. Hollik, and G. Weiglein, *QCD Corrections to the Masses of the Neutral CP-even Higgs Bosons in the MSSM*, *Phys. Rev.* **D58** (1998) 091701, [[hep-ph/9803277](#)].
- [5] S. Heinemeyer, W. Hollik, and G. Weiglein, *Precise Prediction for the Mass of the Lightest Higgs Boson in the MSSM*, *Phys. Lett.* **B440** (1998) 296–304, [[hep-ph/9807423](#)].
- [6] S. Heinemeyer, W. Hollik, and G. Weiglein, *The Masses of the Neutral CP-even Higgs Bosons in the MSSM: Accurate Analysis at the Two-Loop Level*, *Eur. Phys. J.* **C9** (1999) 343–366, [[hep-ph/9812472](#)].
- [7] G. Degrandi, S. Heinemeyer, W. Hollik, P. Slavich, and G. Weiglein, *Towards high-precision predictions for the MSSM Higgs sector*, *Eur. Phys. J.* **C28** (2003) 133–143, [[hep-ph/0212020](#)].
- [8] B. C. Allanach, A. Djouadi, J. L. Kneur, W. Porod, and P. Slavich, *Precise determination of the neutral Higgs boson masses in the MSSM*, *JHEP* **09** (2004) 044, [[hep-ph/0406166](#)].
- [9] J. F. Gunion and H. E. Haber, *The CP-conserving two-Higgs-doublet model: The approach to the decoupling limit*, *Phys. Rev.* **D67** (2003) 075019, [[hep-ph/0207010](#)].
- [10] M. S. Carena and H. E. Haber, *Higgs Boson Theory and Phenomenology. ((V))*, *Prog. Part. Nucl. Phys.* **50** (2003) 63–152, [[hep-ph/0208209](#)].
- [11] B. A. Kniehl, *Radiative Corrections for $H \rightarrow Z Z$ in the Standard Model*, *Nucl. Phys.* **B352** (1991) 1–26.
- [12] B. A. Kniehl, *Radiative Corrections for $H \rightarrow W^+ W^- (\gamma)$ in the Standard Model*, *Nucl. Phys.* **B357** (1991) 439–466.
- [13] J. Kublbeck, M. Bohm, and A. Denner, *Feyn Arts: Computer Algebraic Generation of Feynman Graphs and Amplitudes*, *Comput. Phys. Commun.* **60** (1990) 165–180.

- [14] T. Hahn, *Generating Feynman Diagrams and Amplitudes with FeynArts 3*, *Comput. Phys. Commun.* **140** (2001) 418–431, [[hep-ph/0012260](#)].
- [15] J. Kublbeck, H. Eck, and R. Mertig, *Computer algebraic Generation and Calculation of Feynman Graphs Using FeynArts and FeynCalc*, *Nucl. Phys. Proc. Suppl.* **29A** (1992) 204–208.
- [16] T. Hahn and C. Schappacher, *The Implementation of the Minimal Supersymmetric Standard Model in FeynArts and FormCalc*, *Comput. Phys. Commun.* **143** (2002) 54–68, [[hep-ph/0105349](#)].
- [17] T. Hahn and M. Rauch, *News from FormCalc and LoopTools*, *Nucl. Phys. Proc. Suppl.* **157** (2006) 236–240, [[hep-ph/0601248](#)].
- [18] T. Hahn and J. I. Illana, *Extensions in FormCalc 5.3*, [0708.3652](#).
- [19] T. Hahn, *Generating and Calculating One-loop Feynman Diagrams with FeynArts, FormCalc, and LoopTools*, [hep-ph/9905354](#).
- [20] T. Hahn, S. Heinemeyer, and G. Weiglein, *MSSM Higgs-boson Production at the Linear Collider: Dominant Corrections to the $W W$ Fusion Channel*, *Nucl. Phys.* **B652** (2003) 229–258, [[hep-ph/0211204](#)].
- [21] M. Frank *et al.*, *The Higgs Boson Masses and Mixings of the Complex MSSM in the Feynman-Diagrammatic Approach*, *JHEP* **02** (2007) 047, [[hep-ph/0611326](#)].
- [22] A. Denner, *Techniques for Calculation of Electroweak Radiative Corrections at the One Loop Level and Results for W Physics at LEP-200*, *Fortschr. Phys.* **41** (1993) 307–420, [[0709.1075](#)].
- [23] S. Heinemeyer, W. Hollik, and G. Weiglein, *FeynHiggs: A Program for the Calculation of the Masses of the Neutral CP-even Higgs Bosons in the MSSM*, *Comput. Phys. Commun.* **124** (2000) 76–89, [[hep-ph/9812320](#)].
- [24] T. Hahn, W. Hollik, S. Heinemeyer, and G. Weiglein, *Precision Higgs Masses with FeynHiggs 2.2*, [hep-ph/0507009](#).
- [25] T. Hahn *et al.*, *Higher-order Corrected Higgs Bosons in FeynHiggs 2.5*, *Pramana* **69** (2007) 861–870, [[hep-ph/0611373](#)].
- [26] M. S. Carena, S. Heinemeyer, C. E. M. Wagner, and G. Weiglein, *Suggestions for Improved Benchmark Scenarios for Higgs- boson Searches at LEP2*, [hep-ph/9912223](#).
- [27] M. S. Carena, S. Heinemeyer, C. E. M. Wagner, and G. Weiglein, *Suggestions for Benchmark Scenarios for MSSM Higgs Boson Searches at Hadron Colliders*, *Eur. Phys. J.* **C26** (2003) 601–607, [[hep-ph/0202167](#)].
- [28] W. Hollik and J. H. Zhang, *Radiative corrections to $h^0 \rightarrow WW^*/ZZ^* \rightarrow 4$ leptons in the MSSM*, [[1011.6537](#)].
- [29] **Particle Data Group** Collaboration, W. M. Yao *et al.*, *Review of Particle Physics*, *J. Phys.* **G33** (2006) 1–1232.
- [30] O. Brein and W. Hollik, *Distributions for MSSM Higgs Boson + Jet Production at Hadron Colliders*, *Phys. Rev.* **D76** (2007) 035002, [[0705.2744](#)].
- [31] **ALEPH** Collaboration, S. Schael *et al.*, *Search for Neutral MSSM Higgs Bosons at LEP*, *Eur. Phys. J.* **C47** (2006) 547–587, [[hep-ex/0602042](#)].

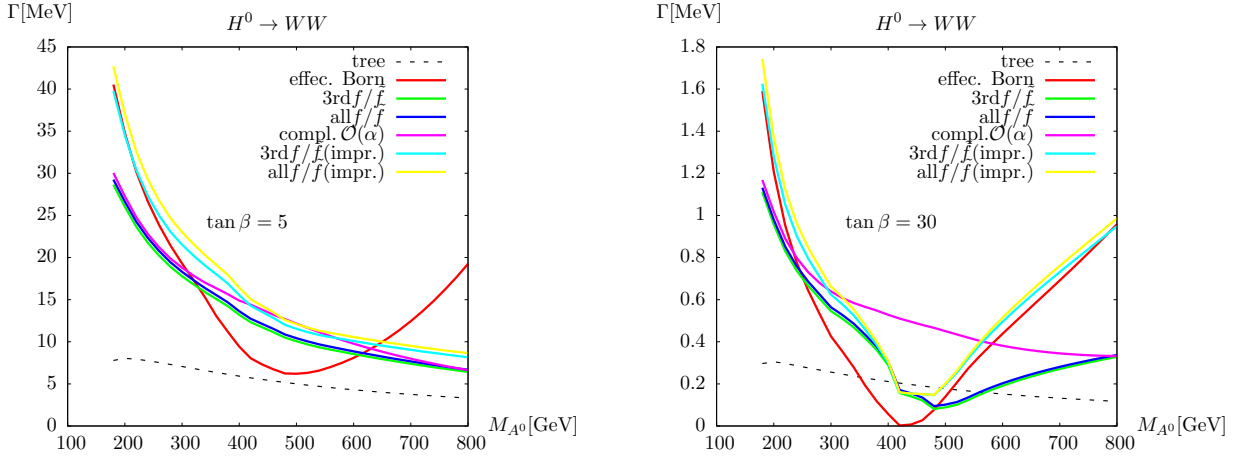


Figure 2: The lowest order and the corrected partial decay widths for $H^0 \rightarrow WW$ as a function of M_{A^0} in the m_h^{\max} scenario for $\tan \beta = 5, 30$, where "effec. Born" denotes the effective Born result, "3rd (all) f/f " denote the results including contributions from the third (all) generation fermions and sfermions, "compl. $\mathcal{O}(\alpha)$ " means the result including the complete $\mathcal{O}(\alpha)$ contribution, "impr." denotes the effective one-loop result.

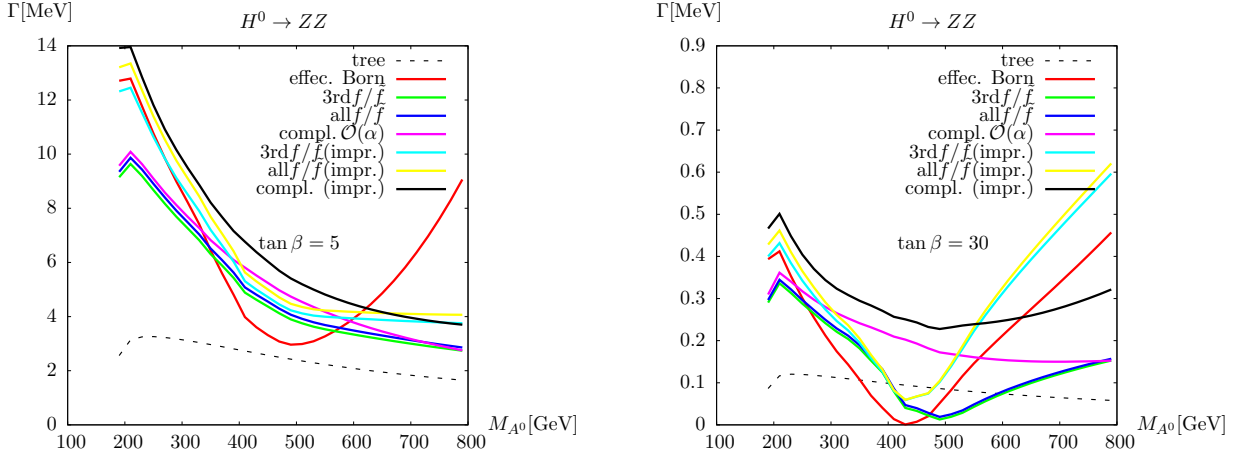


Figure 3: The lowest order and the corrected partial decay widths for $H^0 \rightarrow ZZ$ as a function of M_{A^0} in the m_h^{\max} scenario for $\tan \beta = 5, 30$.

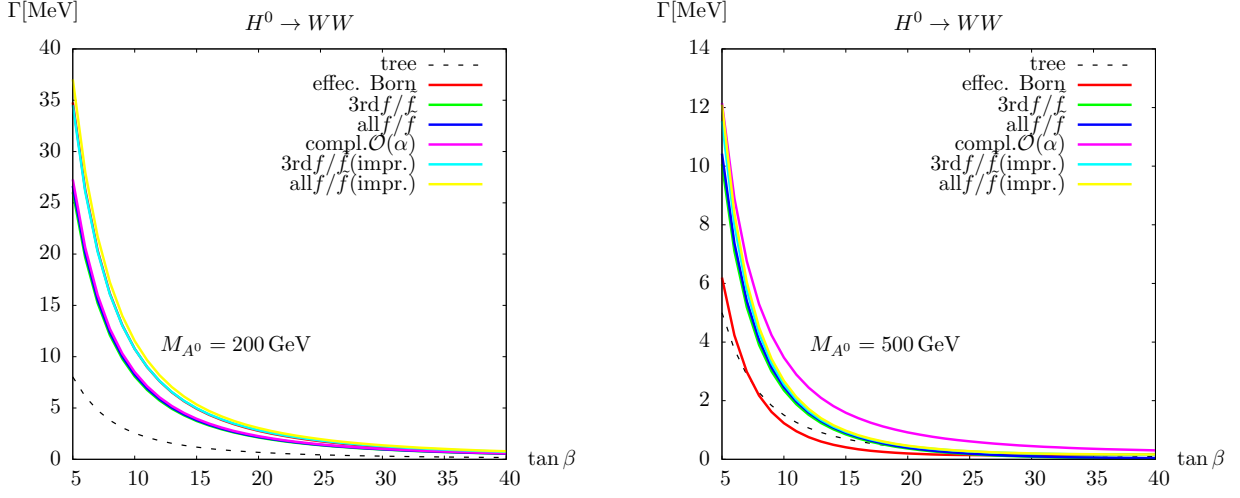


Figure 4: The lowest order and the corrected partial decay widths for $H^0 \rightarrow WW$ as a function of $\tan \beta$ in the m_h^{\max} scenario for $M_{A^0} = 200, 500$ GeV.

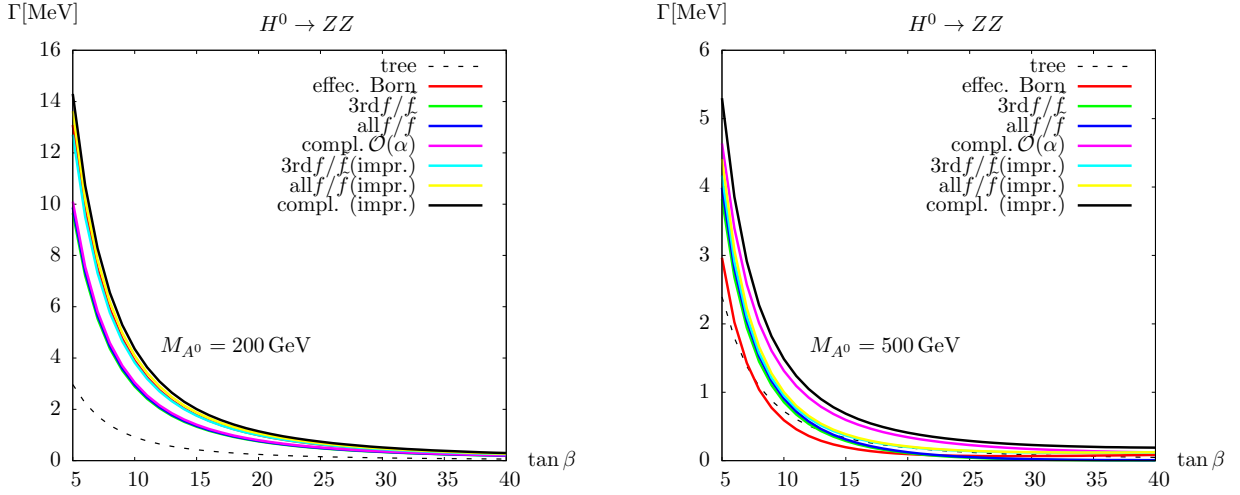


Figure 5: The lowest order and the corrected partial decay widths for $H^0 \rightarrow ZZ$ as a function of $\tan \beta$ in the m_h^{\max} scenario for $M_{A^0} = 200, 500$ GeV.

$$H^0 \rightarrow WW$$

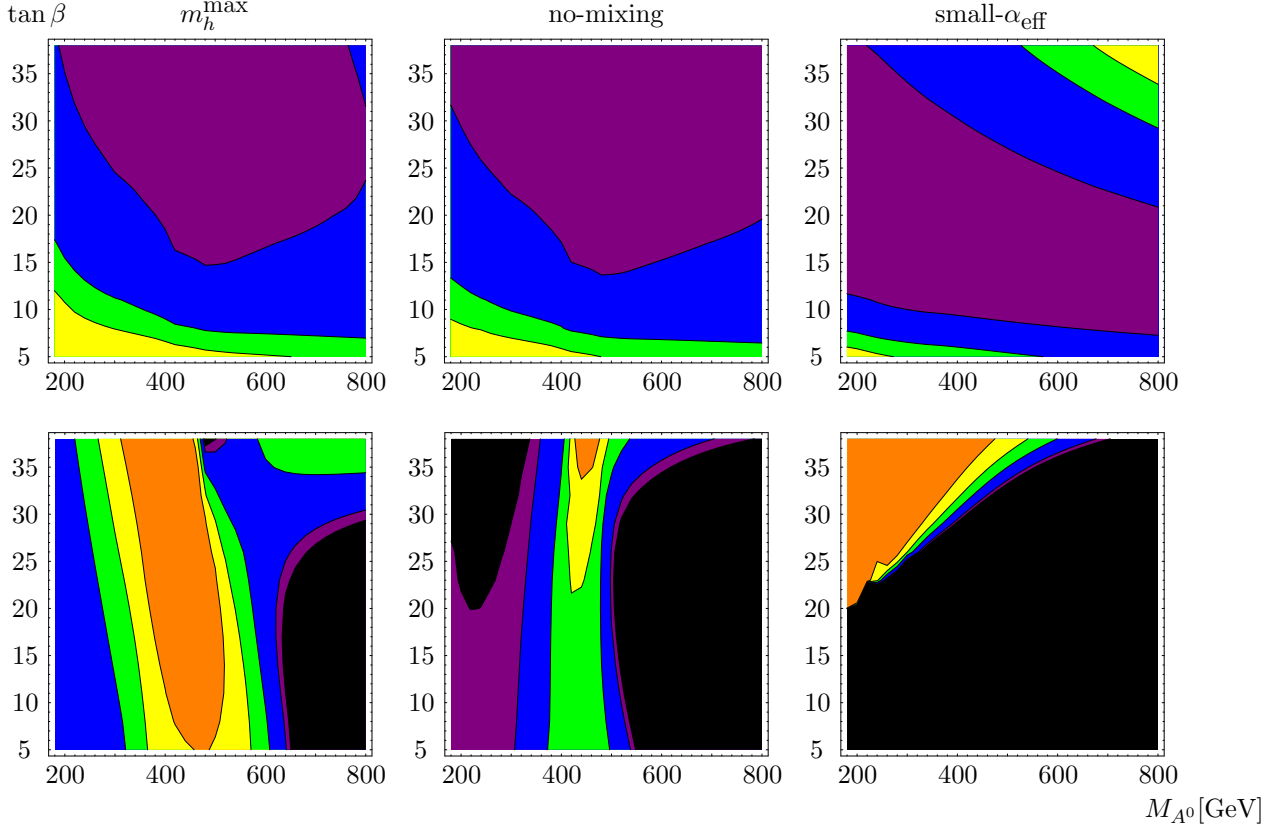


Figure 6: Results for the decay width of $H^0 \rightarrow WW$ in three scenarios. The upper row shows the corrected decay width (effective one-loop result). The purple region corresponds to $\Gamma_{H^0} < 1\text{MeV}$, the blue region to $1\text{MeV} < \Gamma_{H^0} < 5\text{MeV}$, the green region to $5\text{MeV} < \Gamma_{H^0} < 10\text{MeV}$, and the yellow region to $10\text{MeV} < \Gamma_{H^0} < 50\text{MeV}$. The lower row shows the corresponding relative correction δ (divided by the effective Born result). The purple region corresponds to $0 < \delta < 5\%$, the blue region to $5\% < \delta < 25\%$, the green region to $25\% < \delta < 50\%$, the yellow region to $50\% < \delta < 100\%$, and the orange region to $\delta > 100\%$, the black region corresponds to negative relative correction.

$$H^0 \rightarrow ZZ$$

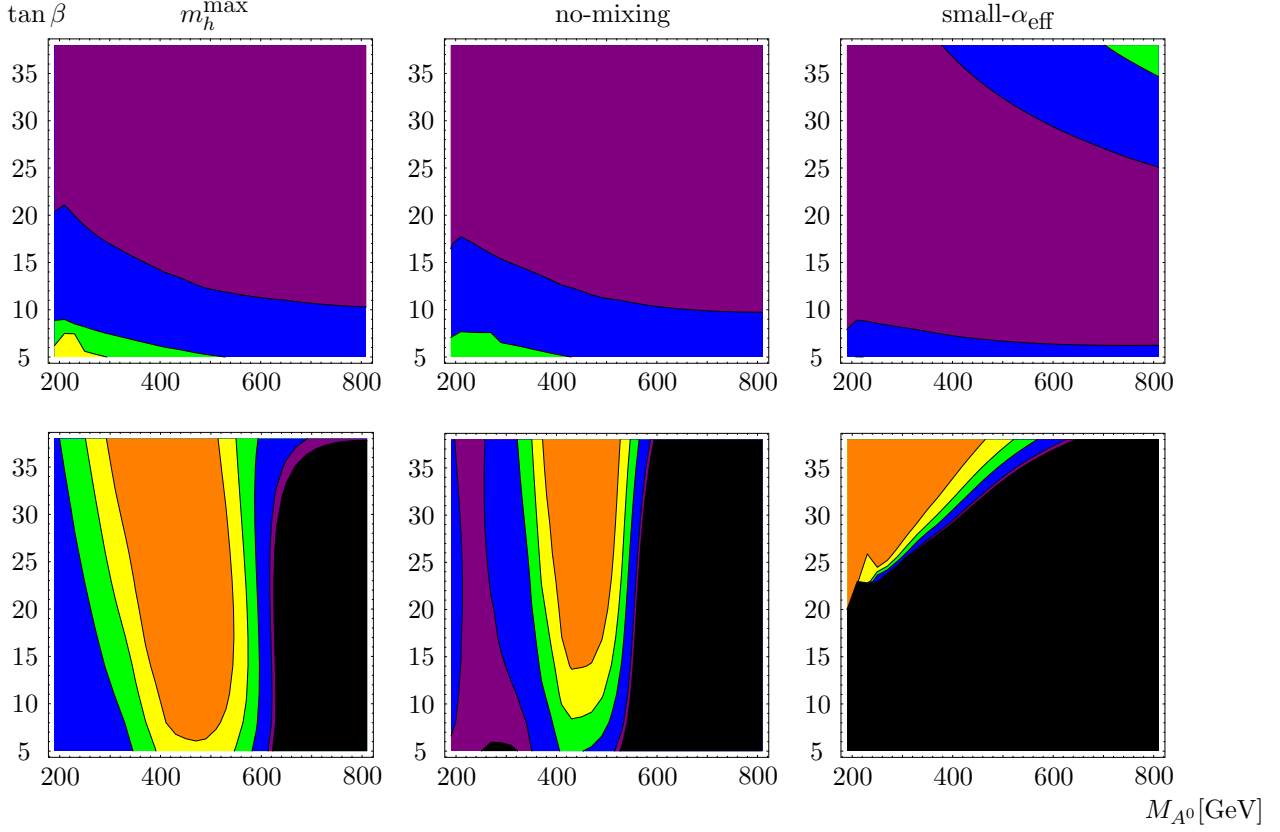


Figure 7: Results for the decay width of $H^0 \rightarrow ZZ$ in three scenarios. The upper row shows the corrected decay width (effective one-loop results). The purple region corresponds to $\Gamma_{H^0} < 1\text{MeV}$, the blue region to $1\text{MeV} < \Gamma_{H^0} < 5\text{MeV}$, the green region to $5\text{MeV} < \Gamma_{H^0} < 10\text{MeV}$, and the yellow region to $10\text{MeV} < \Gamma_{H^0} < 50\text{MeV}$. The lower row shows the corresponding relative correction δ (divided by the effective Born result). The purple region corresponds to $0 < \delta < 5\%$, the blue region to $5\% < \delta < 25\%$, the green region to $25\% < \delta < 50\%$, the yellow region to $50\% < \delta < 100\%$, and the orange region to $\delta > 100\%$, the black region corresponds to negative relative correction.